

Scalable control of graphene growth on 4H-SiC C-face using decomposing silicon nitride masks.

Renaud Puybaret,^{1, 2, a)} John Hankinson,³ James Palmer,³ Clément Bouvier,³ Abdallah Ougazzaden,^{1, 2} Paul L. Voss,^{1, 2} Claire Berger,^{3, 4} and Walt A. de Heer³

¹⁾*School of Electrical and Computer Engineering, Georgia Institute of Technology, 30332, Atlanta, Georgia, USA*

²⁾*Georgia Tech - CNRS UMI 2958, 2-3 Rue Marconi, 57070, Metz, France*

³⁾*School of Physics, Georgia Institute of Technology, 30332, Atlanta, Georgia, USA*

⁴⁾*CNRS-Institute Néel, BP 166, 38042 Grenoble, Cedex 9, France*

(Dated: November 10, 2014)

Patterning of graphene is key for device fabrication. We report a way to increase or reduce the number of layers in epitaxial graphene grown on the C-face (0001) of silicon carbide by the deposition of a 120 nm to 150 nm-thick silicon nitride (SiN) mask prior to graphitization. In this process we find that areas covered by a Si-rich SiN mask have one to four more layers than non-masked areas. Conversely N-rich SiN decreases the thickness by three layers. In both cases the mask decomposes before graphitization is completed. Graphene grown in masked areas show good quality as observed by Raman spectroscopy, atomic force microscopy (AFM) and transport data. By tailoring the growth parameters selective graphene growth and sub-micron patterns have been obtained.

Keywords: graphene, scalable, control, growth, silicon nitride, silicon carbide

Epitaxial graphene (EG) on SiC has great potential for electronics, with compelling physical characteristics such as ballistic transport in nanoribbons¹, half-eV band-gap structures², highly-efficient spin transport³, and ultra-high frequency transistors^{4,5}. Because SiC is a monocrystalline semiconducting industrial substrate, epitaxial graphene on SiC is directly compatible with established scalable device fabrication techniques, making it attractive for advanced electronic devices^{6,7}. Patterning of graphene devices is a key step in the fabrication process. In most cases, 2D graphene is first grown then patterned by oxygen plasma. Selective area growth is a more straightforward approach, as it could in principle provide shaped structures in a single-step process, without relying on the usual post-growth lithography-and-etching steps. Several techniques have been reported for local control of graphene growth. These include in particular AlN capping⁸, ion implantation of Au or Si⁹, the use of amorphous carbon corrals¹⁰, and side-wall nanoribbons¹¹.

In this paper, we report a method for controlling graphene growth selectivity down to the sub-micron level in a one-step process with a vanishing mask. We find that deposition of a 120 nm- to 150 nm-thick silicon nitride mask on C-face (0001) 4H-SiC prior to graphitization modifies the relative number of multi-layer epitaxial graphene (MEG) sheets. The silicon nitride mask decomposes and vanishes before graphitization is complete. Importantly, the stoichiometry of the silicon nitride layers controls whether the silicon nitride layer enhances or suppresses graphene growth relative to uncovered areas.

We find that N-rich silicon nitride masks decrease the average number of layers by three compared to uncovered regions while Si-rich silicon nitride masks increase thickness by two to four layers. The graphene layers of samples prepared with nearly stoichiometric silicon nitride show good mobilities up to $7100 \text{ cm}^2 \cdot \text{V}^{-1} \cdot \text{s}^{-1}$, with electron concentrations in the 10^{12} cm^{-2} range. Raman spectroscopy and AFM measurements confirm that the graphene grown in areas initially covered by the mask has good structural quality.

After preparation of the surface of $3.5 \times 4.5 \text{ mm}^2$ 4H-SiC wafer dies by a high temperature hydrogen etch¹², silicon nitride is deposited by low-power plasma-enhanced chemical vapor deposition (PECVD) using SiH_4 and NH_3 as precursor gases. In Fig. 2, a hard mask (glass slide) covers half the SiC die so that the evaporated SiN layer covers only half the sample. We have confirmed by AFM measurements after removing SiN with hydrofluoric acid (HF) that the plasma does not result in detectable damage to the SiC surface. Patterns of SiN were achieved by standard lithography, using PMMA as the resist, and HF as the etchant (harmless to SiC).

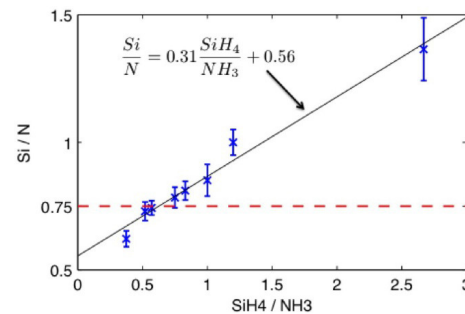


FIG. 1. Calculated ratio of Si over N in the grown SiN film as a function of $\text{SiH}_4 / \text{NH}_3$ precursor ratio used in the PECVD reactor. 0.75 corresponds to stoichiometric Si_3N_4 .

^{a)}Electronic mail: renaudpuybaret@gmail.com

We estimated the stoichiometry of the SiN films as a function of the precursor ratio ($\text{SiH}_4 / \text{NH}_3$) by measuring the refractive index at 632.8 nm ($n_{632.8}$) of the SiN films with an ellipsometer. Following Refs.^{13,14}, $n_{632.8}$ is approximately linearly dependent on the ratio Si/N in the deposited film:

$$\frac{Si}{N} = \frac{n_{632.8} - 1.35}{0.74} \quad (1)$$

The plot of Fig.1 gives a calibration of the SiN composition as a function of the precursor ratio ($\text{SiH}_4 / \text{NH}_3$) in the PECVD process. The straight line is a linear fit of the data.

The confinement-controlled sublimation (CCS) growth method is used for graphitization¹². This technique consists in heating a SiC chip in a graphite enclosure connected to a vacuum chamber (about 10^{-5} mbar) by a calibrated hole. This increases the built-in Si partial pressure, which controls the rate of silicon sublimation from the SiC surface, bringing the graphene growth process close to equilibrium.

The growth process consists of 10 minutes at 800°C , followed by graphene growth between 1450 to 1550°C for 8 to 20 minutes. One exception in Fig.2 is sample Si4, which after the 800°C annealing, was held at 1150°C for 20 minutes, and then graphitized. After graphitization the SiN mask has vanished.

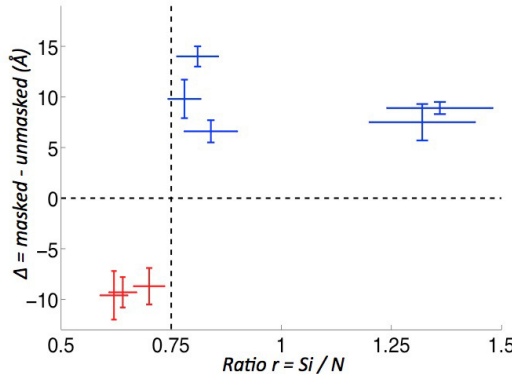


FIG. 2. Local control of thickness as a function of the composition of the silicon nitride film, of stoichiometric formula Si_3N_4 . In blue, Si-rich silicon nitride mask. In red, the mask was N-rich.

Ellipsometry measurements (Horiba Jobin-Yvon AutoSE) on half-masked samples are reported in Fig.2. We used a spot size is $250 \times 250 \mu\text{m}^2$, and analyzed response in the range 440 nm to 850 nm, with a three-term Cauchy model optimized for 4H-SiC and graphene layers¹⁵. Each thickness reported in Fig.2 is the average of 12 measurements, spread on the whole analysed surface. We observe 2 to 3 additional layers of graphene under the Si-rich initially masked (IM) areas, and consistently 3 fewer layers under the N-rich IM areas, compared to the initially bare (IB) half on each sample. Sample Si4 (Si-rich SiN mask), which had an additional higher temperature annealing step at 1150°C , shows 4 to 5 additional graphene layers.

Raman spectra (wavelength is 532 nm) and AFM topography images of samples N1 and Si1 are shown in Figs. 3 and 4, respectively. Of all the samples studied, the silicon nitride films deposited on N1 and Si1 were the closest to stoichiometric Si_3N_4 , cf Fig.2. These samples had the lowest Raman D peaks, sharpest 2D peaks, and smoothest AFM images, and hence were patterned for electronic measurements.

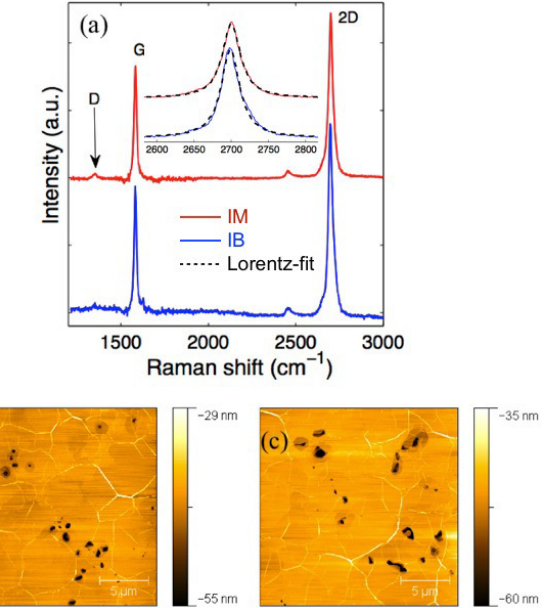


FIG. 3. Sample N1, N-rich SiN mask. (a): Raman spectra (SiC contribution subtracted) of IM and IB areas. (b)-(c): AFM images of (b) IM area and (c) IB area (scale $20 \times 20 \mu\text{m}^2$) showing the typical graphene pleat structure observed in MEG samples.

The Raman spectra of the IM and IB areas of N1 and the IM area of Si1, reveal the characteristic graphene peaks, see Figs. 3 and 4. The graphene 2D and G Raman peaks are clearly identified (the SiC Raman contribution was subtracted). The 2D peak can be fitted by a single Cauchy-Lorentz distribution¹⁶ centered at 2699 cm^{-1} for the IM area of N1 (2700 cm^{-1} and 2689 cm^{-1} , respectively for the IB part of N1 and the IM half of Si1) with $\text{FWHM} = 29 \text{ cm}^{-1}$ (36 cm^{-1} and 29 cm^{-1} , respectively). The D peak at 1350 cm^{-1} is very small, and even undetectable for Si1 and N1. This indicates low defect density in the graphene lattice. For the other samples of Table 1, the 2D peak is centered from 2706 to 2726 cm^{-1} , with FWHM from 52 to 70 cm^{-1} , consistent with 2D MEG^{16,17}. The higher D peaks and the broader blue-shifted 2D peaks (at $\text{FWHM} 52\text{-}70 \text{ cm}^{-1}$) for the other samples referenced in Table 1 reveal respectively smaller domain sizes and compressive strain in the graphene¹⁷. Specifically, we do not observe the characteristic shouldered 2D peak of highly ordered pyrolytic graphite (HOPG), as already reported for multilayered epitaxial graphene on the C-face¹⁶⁻¹⁸. The slight asymmetry of the IB 2D peak in Fig.3(a) may be due to a variation of strain in the graphene stack or a small frac-

tion of Bernal stacking fault¹⁶. MEG and FLG on SiC with a 2D-FWHM of 58 cm^{-1} (ref.⁸), 68 cm^{-1} (ref.¹⁸) and even 71 cm^{-1} (ref.¹⁷) have already been reported.

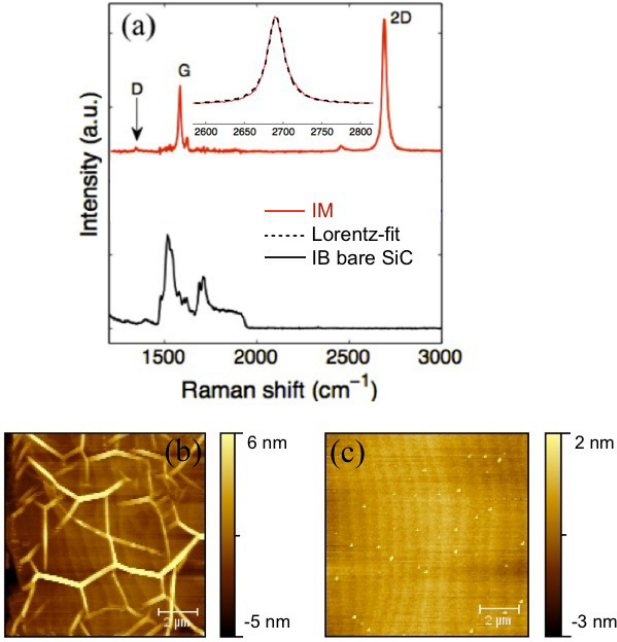


FIG. 4. Sample Si1, Si-rich SiN mask. (a): Raman spectra (SiC contribution subtracted), showing the typical MEG spectrum. For the Raman spectrum the intensity is normalized to the SiC plateau at 1900 cm^{-1} . Note the quasi absence of D-peak. (b)-(c): AFM image of (b) IM area (scale $10\times 10\text{ }\mu\text{m}^2$), and (c) IB area (scale $10\times 10\text{ }\mu\text{m}^2$).

The AFM images of Figs. 3 and 4 confirm the presence of graphene, as shown by the MEG characteristic pleat structure¹². In the graphitized areas, the AFM images in Fig. 3(b)(c) and Fig. 4(b) have a comparable characteristics in terms of pleat structure, including pleat height (1.5-2.4 nm), pleat surface density and semi hexagonal orientation. Sample Si1 is particularly interesting in that while the IM area is fully coated with graphene with an average of 3 layers, the IB area is essentially not graphitized. On the AFM image of Fig. 4(c), a bare SiC step structure can be observed, which is confirmed by Raman spectroscopy, cf Fig.4(a). MEG growth is observed in some spots, most probably initiated at screw dislocations in SiC, as already observed^{19,20}. This indicates selective growth, with graphene where the mask was, and almost no graphene elsewhere.

Hall bars (5 μm long, 3.5 μm wide) were patterned in sample Si1 and N1 using electron beam lithography, oxygen plasma etching and Ti/Pd/Au contacts (thickness 0.5/20/40 nm). From room temperature Hall and magnetoresistance measurements (Fig.5), electronic mobilities are found between 3200 and $7100\text{ cm}^2\text{.V}^{-1}\text{.s}^{-1}$, and carrier concentrations are in the 10^{12} cm^{-2} range, showing excellent graphene quality, as seen in Fig.5.

As a demonstration of the capability of the method, graphene has been selectively grown in the shape of Buzz, Georgia Tech's mascot. Fig.6 demonstrates that the sub-

micrometer resolution of the SiN mask pattern (Fig.6a) is directly transferred to the selectively grown graphene, as shown by optical contrast (Fig.6b) and Raman spectroscopy maps of the characteristic 2D and G graphene peaks. The optical image correlates nicely with the Raman maps, as expected for graphene on SiC²¹. The absence of 2D peak in the grey areas of Fig.6c demonstrates selectivity.

The main result of this study is that the presence of a silicon nitride mask evaporated on silicon carbide prior to graphitization enhances (Si-rich SiN mask) or reduces (N-rich) the number of layers grown compared to uncovered areas. Control samples, with no mask, have the same number of layers (within one layer) as the IB areas under the same growth conditions.

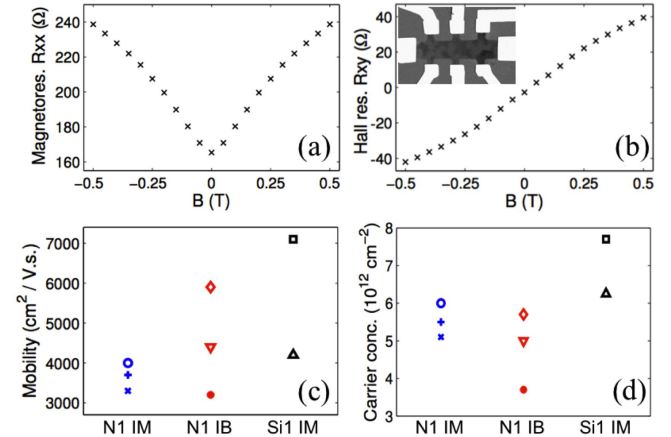


FIG. 5. (a) (b): Magneto- and Hall resistances at room temperature of IM area of Si1: $n=7.7\text{ e}^{12}\text{ cm}^{-2}$ and $\mu=7100\text{ cm}^2\text{.V}^{-1}\text{.s}^{-1}$. Hall bar (SEM picture in the inset) is 3 μm wide. (c) (d): Mobility and carrier concentrations at room temperature measured on the IM area of N1, IB area of N1, and IM area of Si1.

A simple explanation for the reduction of the number of layers under the N-rich masks would be that graphitization is delayed under the mask, starting only after SiN decomposition. It is known that capping SiC with an AlN mask, that doesn't evaporate, prevents graphene formation⁸. More surprising is the enhanced number of layers under the Si-rich mask. A possibility is that Si dangling bonds present in the Si-rich-SiN mask²²⁻²⁵ react with SiC. The role of Si in promoting the growth of graphene was demonstrated by implantation of Si in SiC. The implanted SiC surface results in graphene formation at lower temperature than pristine SiC⁹. Si dangling bonds at SiN_3 sites have already been proposed as the dominant defects in Si-rich and stoichiometric PECVD silicon nitride, acting as amphoteric traps²⁴. Moreover, in N-rich films, electron spin resonance (ESR) studies have shown that the density of these defects is greatly reduced or even suppressed²⁶, making N-rich SiN a better dielectric than Si-rich films. However definitive explanations concerning these processes are still premature, as further experimental evidence is necessary.

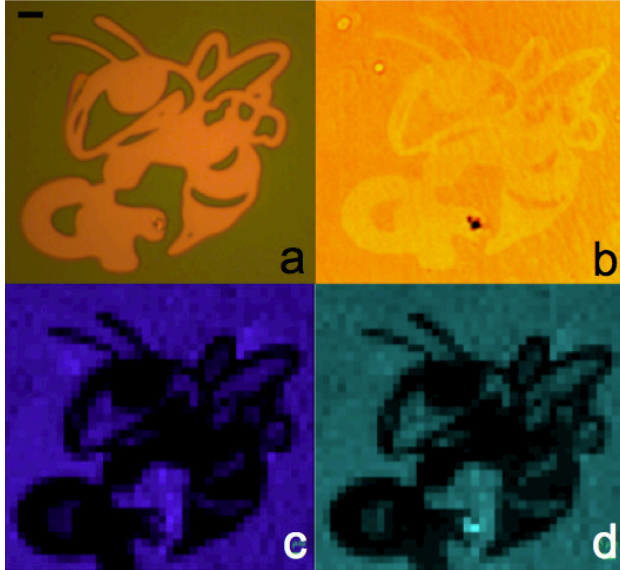


FIG. 6. Buzz-of-principle, MEG on SiC using Si-rich SiN mask, demonstrating sub-micron resolution. a: SiN pattern. b: Subsequent MEG growth on SiC, contrast-enhanced optical image. c: Raman 2D map. d: Raman 2D/G map. Scale bar is 10 μ m.

We have shown that, by using a SiN vanishing mask evaporated onto SiC prior to graphitization, the number of graphene layers varies between masked and non-masked areas. Depending on its chemical composition (Si-rich or N-rich) the SiN mask acts as an enhancer or inhibitor of graphene growth (+/- 3 graphene layers with the present growth conditions). For few layer samples, areas with and without graphene can therefore be produced side by side during the heating process. The mask evaporates during graphene growth so that patterned, mask-free graphene layers are obtained directly in a single heating step. We believe this is a very simple yet potentially quite powerful method to obtain clean patterned graphene structures without the need for post-growth etching.

The authors thank the French Lorraine Region, W. M. Keck Foundation, the National Science Foundation (DMR-0820382), the Air Force Office of Scientific Research for financial support and the Partner University Fund for a travel grant. We also acknowledge funding from the Graphene Flagship European program. At last my special thanks to J. P. Turmaud, X. Yang, A. Savu, Y. Hu, F. Zaman, S. Bryan, R. Dong, T. Guo, M. Ruan, B. Zhang, M. Sprinkle, J. Hicks, O. Vail, Y. El Gmili, N. Devlin, C. Chapin and D. Brown for training, technical support and fruitful discussions.

¹J. Baringhaus, M. Ruan, F. Edler, A. Tejeda, M. Sicot, A. Taleb-Ibrahimi, A.-P. Li, Z. Jiang, E. H. Conrad, C. Berger, C. Tegenkamp, and W. A. de Heer, “Exceptional ballistic transport in epitaxial graphene nanoribbons,” *Nature*, vol. 506, no. 7488, pp. 349–354, 2014.

²J. Hicks, A. Tejeda, A. Taleb-Ibrahimi, M. S. Nevius, F. Wang, K. Shepperd, J. Palmer, F. Bertran, P. Le Fevre, J. Kunc, W. A. de Heer, C. Berger, and E. H. Conrad, “A wide-bandgap

metal-semiconductor-metal nanostructure made entirely from graphene,” *Nature Physics*, vol. 9, no. 1, pp. 49–54, 2013.

³B. Dlbak, M.-B. Martin, C. Deranlot, B. Servet, S. Xavier, R. Mattana, M. Sprinkle, C. Berger, W. A. De Heer, F. Petroff, A. Anane, P. Seneor, and A. Fert, “Highly efficient spin transport in epitaxial graphene on SiC,” *Nature Physics*, vol. 8, no. 7, pp. 557–561, 2012.

⁴Y. M. Lin, C. Dimitrakopoulos, K. A. Jenkins, D. B. Farmer, H. Y. Chiu, A. Grill, and P. Avouris, “100-GHz Transistors from Wafer-Scale Epitaxial Graphene,” *Science*, vol. 327, no. 5966, p. 662, 2010.

⁵Z. Guo, R. Dong, P. S. Chakraborty, N. Lourenco, J. Palmer, Y. Hu, M. Ruan, J. Hankinson, J. Kunc, J. D. Cressler, C. Berger, and W. A. de Heer, “Record Maximum Oscillation Frequency in C-Face Epitaxial Graphene Transistors,” *Nano Letters*, vol. 13, no. 3, pp. 942–947, 2013.

⁶C. Berger, Z. Song, T. Li, X. Li, A. Ogbazghi, R. Feng, Z. Dai, A. Marchenkov, E. Conrad, P. First, and W. de Heer, “Ultrathin epitaxial graphite: 2D electron gas properties and a route toward graphene-based nanoelectronics,” *Journal of Physical Chemistry B*, vol. 108, no. 52, pp. 19912–19916, 2004.

⁷Y.-M. Lin, A. Valdes-Garcia, S.-J. Han, D. B. Farmer, I. Meric, Y. Sun, Y. Wu, C. Dimitrakopoulos, A. Grill, P. Avouris, and K. A. Jenkins, “Wafer-Scale Graphene Integrated Circuit,” *Science*, vol. 332, no. 6035, pp. 1294–1297, 2011.

⁸M. Rubio-Roy, F. Zaman, Y. Hu, C. Berger, M. Moseley, J. Meindl, and W. de Heer, “Structured epitaxial graphene growth on SiC by selective graphitization using a patterned AlN cap,” *Applied Physics Letters*, vol. 96, no. 8, 2010.

⁹S. Tongay, M. Lemaitre, J. Fridmann, A. F. Hebard, B. P. Gila, and B. R. Appleton, “Drawing graphene nanoribbons on SiC by ion implantation,” *Applied Physics Letters*, vol. 100, no. 7, 2012.

¹⁰J. Palmer, J. Kunc, Y. Hu, J. Hankinson, Z. Guo, C. Berger, and W. A. de Heer, “Controlled epitaxial graphene growth within removable amorphous carbon corrals,” *Applied Physics Letters*, vol. 105, no. 2, 2014.

¹¹M. Sprinkle, M. Ruan, Y. Hu, J. Hankinson, M. Rubio-Roy, B. Zhang, X. Wu, C. Berger, and W. A. de Heer, “Scalable templated growth of graphene nanoribbons on SiC,” *Nature Nanotechnology*, vol. 5, no. 10, pp. 727–731, 2010.

¹²W. de Heer, C. Berger, M. Ruan, M. Sprinkle, X. Li, Y. Hu, B. Zhang, J. Hankinson, and E. Conrad, “Large area and structured epitaxial graphene produced by confinement controlled sublimation of silicon carbide,” *Proceedings of the National Academy of Sciences*, vol. 108, no. 41, pp. 16900–16905, 2011.

¹³N. Piggins, E. Davis, and S. Bayliss, “Optical properties and spin densities of SiNx(-H) films,” *Journal of Non-Crystalline Solids*, vol. 97-8, no. Part 2, pp. 1047–1050, 1987.

¹⁴W. Claassen, W. Valkenburg, F. Habraken, and Y. Tamminga, “Characterization of plasma silicon-nitride layers,” *Journal of the Electrochemical Society*, vol. 130, no. 12, pp. 2419–2423, 1983.

¹⁵“Average thicknesses obtained by ellipsometer match other thickness measurements, notably light absorption. to be published.”

¹⁶C. Faugeras, A. Neriere, M. Potemski, A. Mahmood, E. Du-jardin, C. Berger, and W. A. de Heer, “Few-layer graphene on SiC, pyrolytic graphite, and graphene: A Raman scattering study,” *Applied Physics Letters*, vol. 92, no. 1, 2008.

¹⁷J. Roehrl, M. Hundhausen, K. V. Emtsev, T. Seyller, R. Graupner, and L. Ley, “Raman spectra of epitaxial graphene on SiC(0001),” *Applied Physics Letters*, vol. 92, no. 20, 2008.

¹⁸N. Sharma, D. Oh, H. Abernathy, M. Liu, P. N. First, and T. M. Orlando, “Signatures of epitaxial graphene grown on Si-terminated 6H-SiC (0001),” *Surface Science*, vol. 604, no. 2, pp. 84–88, 2010.

¹⁹Y. Hu, M. Ruan, Z. Guo, R. Dong, J. Palmer, J. Hankinson, C. Berger, and W. A. de Heer, “Structured epitaxial graphene: growth and properties,” *Journal of Physics D-Applied Physics*, vol. 45, no. 15, SI, 2012.

²⁰J. K. Hite, M. E. Twigg, J. L. Tedesco, A. L. Friedman, R. L. Myers-Ward, C. R. Eddy, Jr., and D. K. Gaskill, “Epitaxial

Graphene Nucleation on C-Face Silicon Carbide,” *Nano Letters*, vol. 11, no. 3, pp. 1190–1194, 2011.

²¹A. Tiberj, N. Camara, P. Godignon, and J. Camassel, “Micro-Raman and micro-transmission imaging of epitaxial graphene grown on the Si and C faces of 6H-SiC,” *Nanoscale Research Letters*, vol. 6, 2011.

²²J. Robertson, “Defect and impurity states in silicon nitride,” *Journal of Applied Physics*, vol. 54, no. 8, pp. 4490–4493, 1983.

²³J. Robertson and M. Powell, “Gap states in silicon nitride,” *Applied Physics Letters*, vol. 44, no. 4, pp. 415–417, 1984.

²⁴W. Lau, S. Fonash, and J. Kanicki, “Stability of electrical properties of nitrogen-rich, silicon-rich, and stoichiometric silicon nitride films,” *Journal of Applied Physics*, vol. 66, no. 6, pp. 2765–2767, 1989.

²⁵W. Warren, J. Robertson, and J. Kanicki, “Si and N dangling bond creation in silicon nitride thin films,” *Applied Physics Letters*, vol. 63, no. 19, pp. 2685–2687, 1993.

²⁶D. Jousse, J. Kanicki, D. Krick, and P. Lenahan, “Electron spin resonance study of defects in plasma-enhanced chemical vapor-deposited silicon-nitride,” *Applied Physics Letters*, vol. 52, no. 6, pp. 445–447, 1988.